Hindawi Publishing Corporation
Journal of Nanomaterials
Volume 2016, Article ID 7083284, 9 pages
http://dx.doi.org/10.1155/2016/7083284

Research Article

Influence of the Total Gas Flow at Different Reaction Times for CVD-Graphene Synthesis on Polycrystalline Nickel

M. P. Lavin-Lopez, J. L. Valverde, L. Sanchez-Silva, and A. Romero

Department of Chemical Engineering, University of Castilla-La Mancha, Avenida Camilo Jose Cela 12, 13071 Ciudad Real, Spain

Correspondence should be addressed to M. P. Lavin-Lopez; mariadelprado.lavin@uclm.es and A. Romero; amaya.romero@uclm.es

Received 30 December 2015; Revised 31 March 2016; Accepted 11 April 2016

Academic Editor: Shu Seki

Optimization of the total gas flow (CH_4+H_2) during the reaction step for different reaction times for CVD-graphene synthesis on polycrystalline nickel foil using an atmospheric pressure set-up is reported. A *thickness value* related to number of graphene layers in each of the synthesized samples was determined using an Excel-VBA application. This method assigned a *thickness value* between 1 and 1000 and provided information on the percentage of each type of graphene (monolayer, bilayer, and multilayer) deposited onto the polycrystalline nickel sheet. The influence of the total gas flow during the reaction step and the reaction time was studied in detail. Optical microscopy showed that samples were covered with different types of graphene, such as multilayer, few-layer, bilayer, and monolayer graphene. The synthesis variables were optimized according to the *thickness value* and the results were verified by Raman spectroscopy. The best conditions were obtained with a reaction temperature of 980°C, a CH_4/H_2 flow rate ratio of 0.07 v/v, a reaction time of 1 minute, and a total gas flow of 80 NmL/min. In the sample obtained under the optimized conditions, 80% of the area was covered with monolayer graphene and less than 1% with multilayer graphene.

1. Introduction

Graphene can be defined as a 2D carbon network with a hexagonal crystal structure of sp^2-bonded atoms. Graphene has attracted a great deal of attention due to its exceptional properties [1–5], which make it an outstanding material for a wide variety of applications such as transparent conductive films, composites, batteries, and solar cells [6].

Two different strategies can be employed to synthesize graphene: *top down and bottom up*. Top down strategies include those methods in which graphite is attacked by liquid or mechanical procedures to synthesize graphene. This strategy includes the following methods: *Micromechanical Cleavage* [1, 7, 8], *Exfoliation of Graphite Intercalation Compounds (GICs)* [9], *Arc Discharge* [10, 11], *Unzipping Carbon Nanotubes (CNTs)* [12, 13], *Graphene Oxide Exfoliation* [7], and *Solvent-Based Exfoliation* [14, 15]. The bottom up strategy concerns those methods that use a carbonaceous source to synthesize graphene. The principal methods included in the bottom up strategy are *epitaxial growth on Silicon Carbide (SiC)* [7, 16] and *Chemical Vapor Deposition (CVD)* [17, 18].

Chemical Vapor Deposition can be defined as a method in which a carbonaceous source reacts at high temperature using a transition metal as a catalyst. This metal is involved in both the decomposition of the carbon species and the nucleation of the graphene lattice. The transition metals that are most commonly used to synthesize graphene are nickel and copper [19], although other transition metals have also been used, for example, Ru, Co, and Pt [20, 21].

The solubility of carbon in copper is extremely low, at least 100 times lower than in nickel. Consequently, graphene is grown by superficial diffusion in the case of copper, whereas in the case of nickel graphene is grown by carbon segregation followed by precipitation [22]. In other words, the growth mechanism for graphene on copper is based on a superficial catalytic reaction in which metallic substrates are exposed to hydrocarbons. The hot metal surface acts as a catalyst, thus allowing the thermal decomposition of hydrocarbons

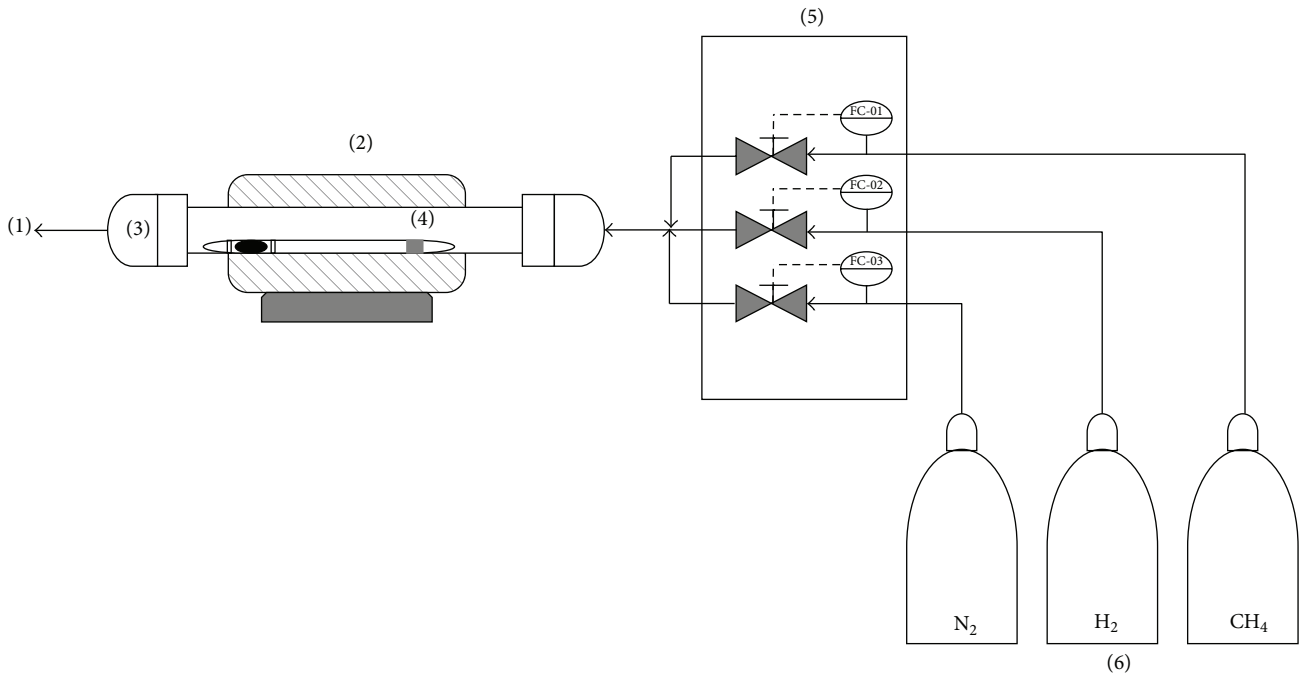

(1) Gases outside system
(2) Furnace
(3) Quartz tube
(4) Nickel sheet
(5) Gases control system
(6) Gases supply system

Figure 1: Set-up used for the CVD synthesis of graphene on polycrystalline nickel.

in the metal to form a solution, which after saturation leads to the formation of graphite. On cooling the sample, the carbon atoms dissolve in the metal to form graphene layers [17]. In the case of Ni, graphene growth occurs after gas decomposition. Carbon atoms diffuse through the metal surface to form a solid solution. Carbon atoms subsequently segregate from the metal at the metal surface and then precipitate to form graphene sheets [23].

Lavin-Lopez et al. [23] reported that graphene growth on transition metals is largely influenced by several factors, which include the synthesis temperature, synthesis time, and CH_4/H_2 flow rate ratio. The researchers defined the *thickness value* as a value calculated by a homemade Excel-VBA application designed to control the graphene thickness. This value can range between 1 and 1000, depending on the number of graphene layers and the percentage of each type of graphene (monolayer, bilayer, few-layer, and multilayer) deposited over the sample. Low temperatures (e.g., 980°C) and low CH_4/H_2 flow rate ratios (e.g., 0.07 v/v) were required to synthesize high quality graphene. Monolayer, bilayer, few-layer, and multilayer graphene were obtained on polycrystalline nickel, with a maximum thickness value of 781 and around 76% of the sheet covered by monolayer graphene.

The aim of the work described here was to optimize CVD-graphene growth on polycrystalline nickel sheets using an atmospheric pressure set-up. The total gas flow applied during the reaction step (CH_4+H_2) at different reaction times was studied in detail. H_2 and N_2 were used as the carrier gases and the former was also used as the reduction gas. CH_4 was used as the precursor gas.

2. Experimental

2.1. Materials. Polycrystalline nickel sheets (25 μm thick) with a purity of 99.99% were purchased from GOODFELLOW Cambridge Ltd. Hydrogen and nitrogen with a purity of 99.999% and methane with a purity of 99.5% were supplied by Praxair España Ltd.

2.2. Method. Graphene samples were grown at atmospheric pressure on 25 μm thick polycrystalline nickel foil in a 40-inch quartz tube heated by a furnace (Figure 1) using the CVD method [24]. The furnace was heated to 900°C by passing a flow of H_2 (100 sccm) and N_2 (400 sccm) through it in order to prevent oxidation of the polycrystalline nickel sheet. The furnace was maintained at this temperature for 45 minutes to perform the reduction step by annealing the polycrystalline nickel sheet. The temperature set point was increased to 980°C and a mixture of methane and hydrogen in a ratio of 0.07 v/v was introduced for different times (in the range of 15 min to 30 s) to complete the reaction step. The total flow during the reaction step was varied in the range of 80–130 NmL/min. Finally, the system was cooled down (10°C min^{-1}) in a flow of nitrogen (400 sccm). The synthesis process is summarized in Figure 2.

2.3. Characterization

2.3.1. Raman Spectroscopy. A SENTERRA Raman spectrophotometer with 600 lines per mm grating and 532 nm laser wavelength at a very low laser power (<1 mW) to avoid

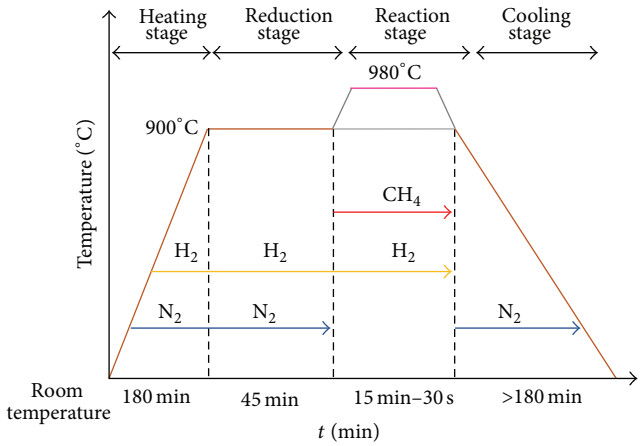

FIGURE 2: Summary of the stage times, temperatures, and gases used during the CVD-graphene synthesis process.

any heating effect was used to characterize the different graphene samples.

The D peak, which is visible at ~1350 cm^{-1}, is related to the presence of defects (edges, dislocations, cracks, or vacancies) in graphitic materials [25]. Two more peaks, which are denoted as G and 2D bands, are visible at around 1580–1620 cm^{-1} and ~2700 cm^{-1}, respectively. The G peak is due to the symmetry-allowed graphite band and provides a way to assess the vibration in the plane of sp^2 hybridized carbon atoms that form the graphene sheets [25]. The 2D peak is the hallmark of different numbers of graphene layers [26, 27].

The level of defects present in graphene samples can be quantified by measuring the intensity ratio of the D and G bands (I_D/I_G). On the other hand, the number of graphene layers is directly related to the ratio of the G and 2D bands (I_{2D}/I_G). Other notable parameters in the characterization of graphene are *FWHM* (Full Width at Half Maximum) and *2D and G peak position* (Raman shift, cm^{-1}). FWHM is related to the lifetime of the excited states (lifetime for the Raman scattering process), which is calculated as the Raman shift difference to the half-average height of the 2D band. A variation in the position of G peak can be attributed to electronic doping between the graphene and the substrate [28]. Finally, the position of the *2D peak* in the Raman spectrum of graphene should be displaced to lower Raman shift values when compared to that in the Raman spectrum of graphite (ranging from 2710 to 2720 cm^{-1}) [29].

2.3.2. Optical Microscopy. A SENTERRA X50 microscope in conjunction with the software OPUS was used to analyze the graphene samples. About 50 photomicrographs (132.4 μm ∗ 98.53 μm) were analyzed (although only six of them were considered as representative to be shown). In each image, four different colors were detected. It was confirmed that a dark orange color would correspond to multilayer graphene, a pale orange color was associated with few-layers graphene, a yellow color would correspond to bilayer graphene, and white areas were associated with monolayer graphene.

2.3.3. Determination of the Graphene Thickness Value. An in-house Excel-VBA software application was designed with the aim of controlling the graphene thickness. This software was able to evaluate the percentages of the different types of graphene present on a polycrystalline nickel foil by evaluating the different colors in digitalized photomicrographs. It was clearly demonstrated by Raman spectroscopy that the different colors in the photomicrographs were related to different types of graphene (Figure 3). The Excel-VBA software application allowed the percentage of each type of graphene (multilayer, few-layer, bilayer, and monolayer graphene) to be evaluated by assessing the corresponding colors in the photomicrographs. For this purpose, a logarithmic scale (similar to that used to represent the pH in liquids) was considered. Thus, values of 1, 10, 100, and 1000 were assigned to multilayer, few-layer, bilayer, and monolayer graphene, respectively. The *thickness value* of the sheet was calculated as an average of the percentage obtained for each type of graphene [17].

3. Results

In order to analyze the influence that the total gas flow (CH_4+H_2) during the reaction step at different reaction times (15 min–30 s) has on the main characteristics of the synthesized graphene, different experiments were carried out by varying the flow between 130 NmL/min and 80 NmL/min. The other operational parameters, such as reaction temperature and CH_4/H_2 flow rate ratio, were optimized in previous studies and were kept constant when assessing the influence of total gas flow during reaction step at different reaction times. The synthesis conditions were as follows: reaction temperature, 980°C; reaction time, 15 min–30 s; CH_4/H_2 flow rate ratio, 0.07 v/v; and total gas flow (CH_4+H_2), 80–130 NmL (CH_4+H_2)/min [23]. According to previous studies and the experimental result obtained, two different steps could be distinguished in the CVD-graphene growth mechanism over polycrystalline nickel. The first one was associated with the absorption of carbon atoms into the nickel substrate. The second one comprises the outdiffusion and adsorption of these carbon atoms to the nickel surface [23, 30].

The images obtained by optical microscopy for a total gas flow (CH_4+H_2) of 130 NmL/min (a), 100 NmL/min (b), and 80 NmL/min (c) for different reaction times are shown in Figure 4. It can be seen that four different colors can be distinguished over the sample. For all the total gas (CH_4+H_2) flows applied during the reaction step, darker orange colors were mainly observed at higher reaction times. In this way, multilayer and few-layer graphene, which correspond to the darker and paler orange colors, respectively, covered the samples synthesized with longer reaction times (>5 min) due to the longer exposure of the nickel foil to the carbonaceous source. In contrast, optical microscopy images corresponding to nickel sheets exposed for shorter times to the carbonaceous gas were lighter in color. In this way, samples synthesized at lower reaction time (<3 min) were mostly covered with yellow and white areas, which correspond with bilayer and monolayer graphene, respectively.

The effects that the total gas flow (at different reaction times) had on the thickness value of graphene deposited on

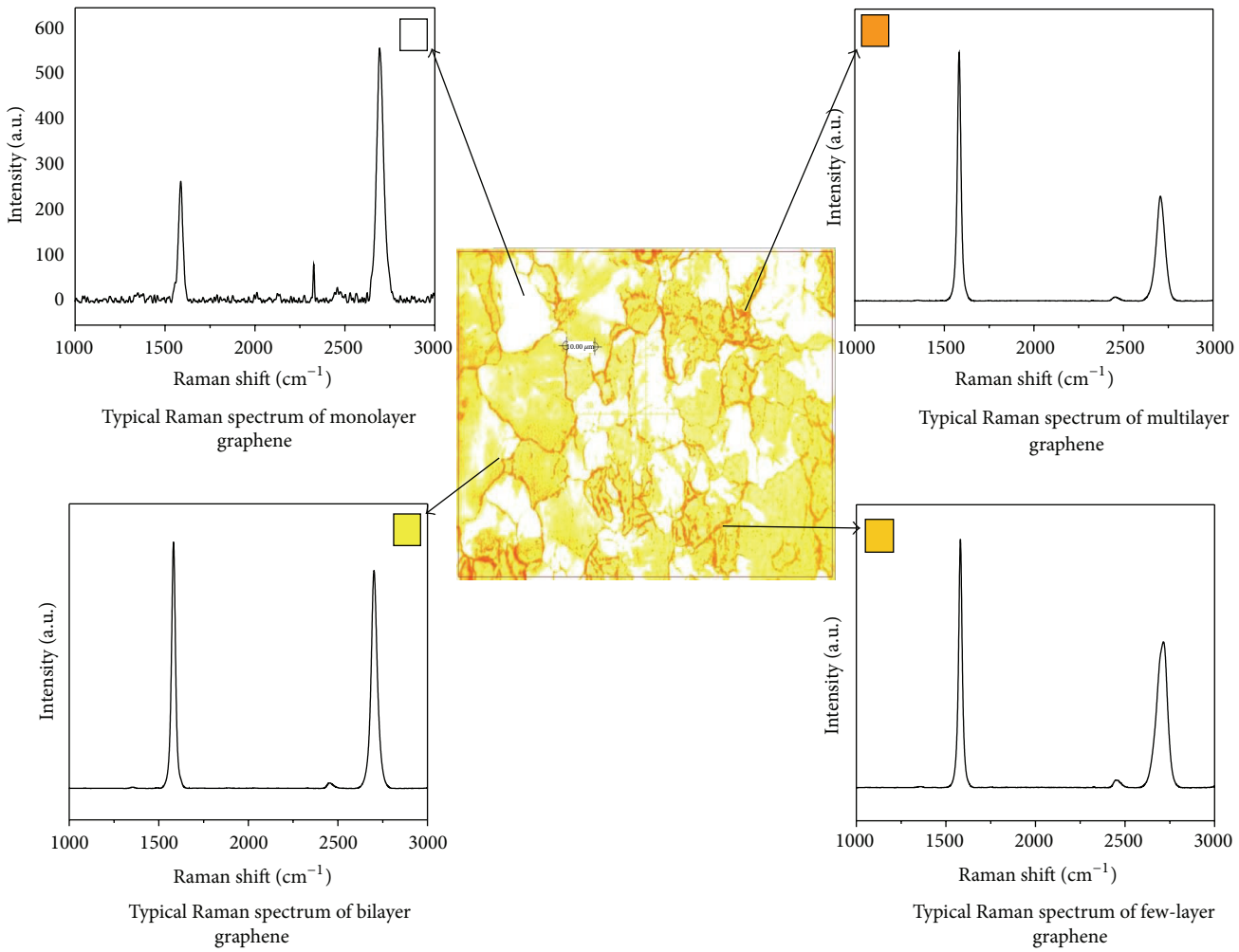

Figure 3: Optical microscopy images (Raman spectroscopy): relationship between the different colors and the type of graphene.

the polycrystalline nickel foil are summarized in Figure 5. A maximum thickness value was obtained for each total gas flow (CH_4+H_2) studied. In all cases, a reaction time of 1 minute gave the highest thickness value and this was therefore considered the optimum reaction time. Lower thickness values were obtained with higher reaction times because the longer exposure to the carbonaceous source led to the formation of higher numbers of graphene layers and, consequently, to a lower *thickness value* [23]. On employing a reaction time of 30 seconds, the thickness value decreased because there was insufficient time to allow homogeneous graphene growth over the entire sample. This led to the presence of zones without graphene on the polycrystalline metal.

Furthermore, an increase in the thickness value on decreasing the total gas flow (CH_4+H_2) applied during the reaction step can be observed. In this way, the lowest thickness value (781) was obtained for a total gas flow of 130 NmL/min. This thickness value increased to 798 on using a total gas flow of 100 NmL/min. Finally, the highest thickness value was 810 and this corresponds to a total gas flow of 80 NmL/min. Therefore, a low total gas flow (CH_4+H_2), that is, 80 NmL/min, was considered to be optimum.

Six representative optical microscopy images for the optimum total gas flow (CH_4+H_2) applied during reaction step (80 NmL/min) for the optimum total time (1 minute) are shown in Figure 6. The results obtained for these samples are given in Table 1. Most of the samples (around 80%) were covered with monolayer graphene, which corresponds to white areas in the photomicrographs. Multilayer graphene on the polycrystalline nickel foil was present at less than 1%. The rest of the sample was covered with few-layer and bilayer graphene, with the percentage of these graphene varying in the range from 18 to 5%.

In an effort to corroborate the optimum results obtained, Raman spectroscopy was used to characterize the graphene samples synthesized; this technique is considered to be a reliable and quick method to characterize graphene [25, 29, 31, 32]. The main characteristic Raman parameters are listed in Table 2 for samples synthesized under 1-minute reaction time with different total gas flow (CH_4+H_2) applied during the reaction step.

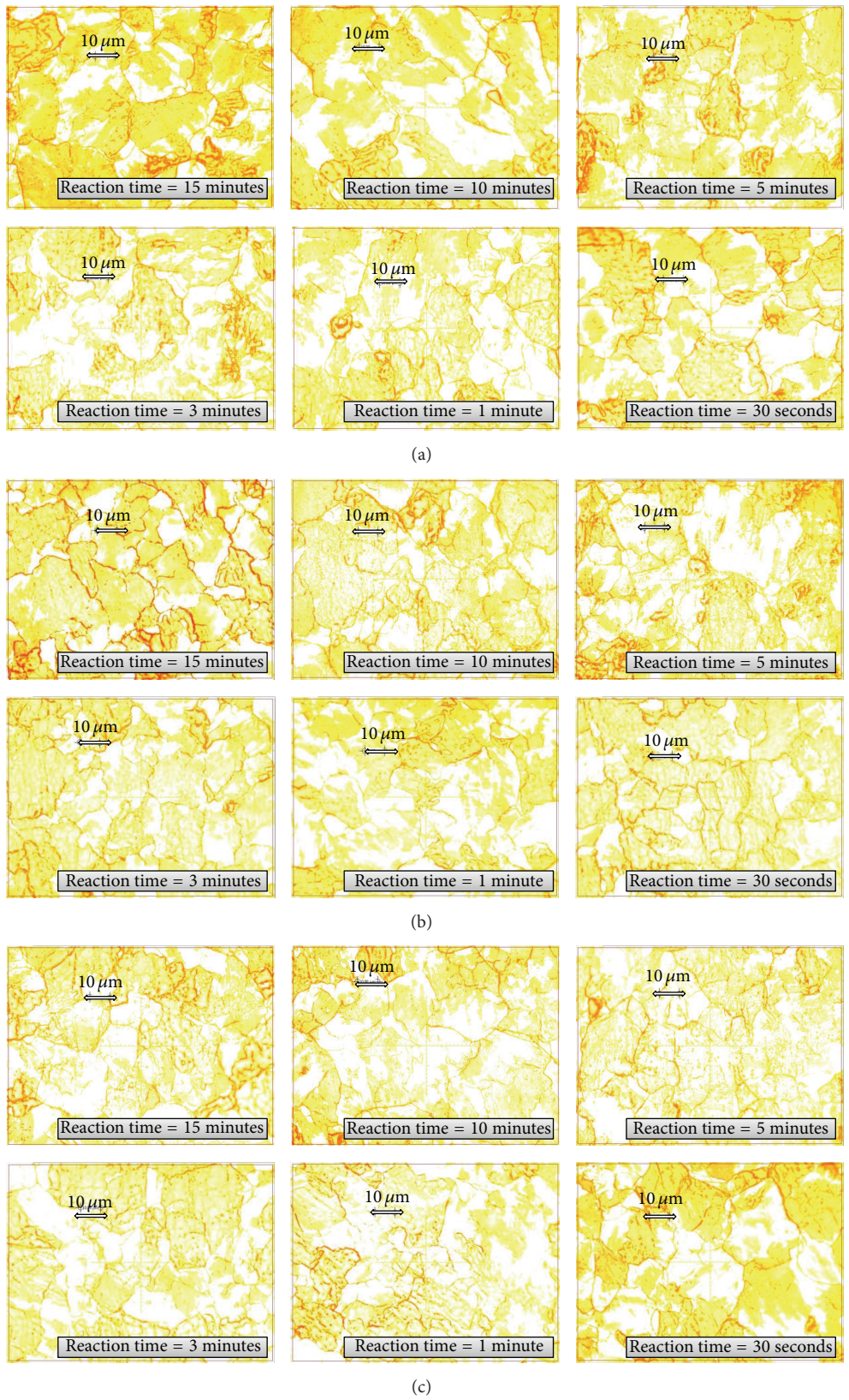

FIGURE 4: Optical microscopy images: total gas flow during reaction step of (a) 130 NmL/min, (b) 100 NmL/min, and (c) 80 NmL/min (synthesis conditions: 980°C, 15 min–30 s reaction time, CH_4/H_2 = 0.07 v/v, 130–80 NmL (CH_4+H_2)/min).

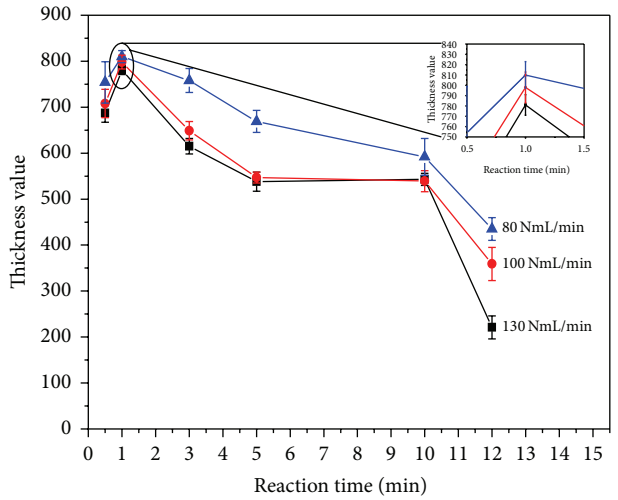

Figure 5: Graphene *thickness value* versus *time* (synthesis conditions: 980°C, 15 min–30 s reaction time, CH_4/H_2 = 0.07 v/v, 80–130 NmL (CH_4+H_2)/min).

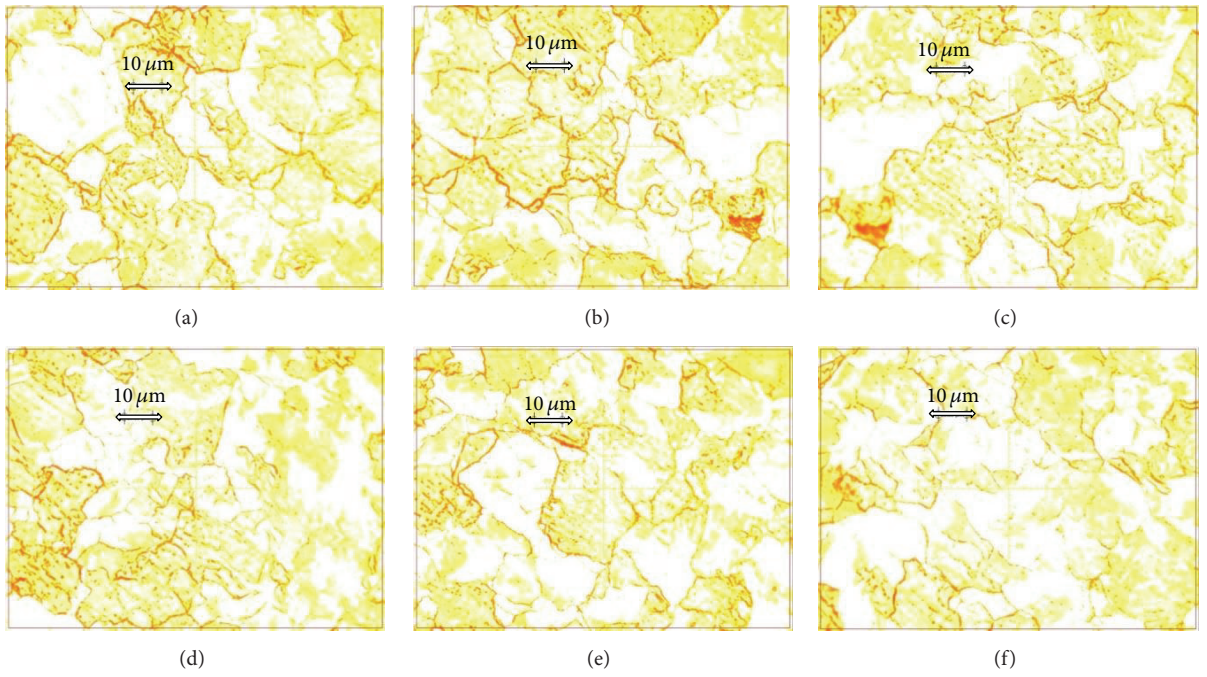

Figure 6: Optical microscopy images corresponding to the optimized graphene sample (synthesis conditions: 980°C, 1 min reaction time, CH_4/H_2 = 0.07 v/v, 80 NmL (CH_4+H_2)/min).

Table 1: Percentage of each type of graphene and *thickness values* corresponding to the optimized graphene sample.

Images	Multilayer graphene (%)	Few-layer graphene (%)	Bilayer graphene (%)	Monolayer graphene (%)	Thickness value
1	0.21	12.62	9.04	78.13	792
2	0.97	18.08	11.22	69.73	710
3	0.36	8.40	7.46	83.88	847
4	0.28	13.76	9.75	76.21	773
5	0.11	8.93	7.59	83.36	842
6	0.05	5.15	5.42	89.38	899

(Synthesis conditions: 980°C, 1 min reaction time, CH_4/H_2 = 0.07 v/v, and 80 NmL (CH_4 + H_2)/min).

Table 2: Raman spectroscopy parameters and percentage of each type of graphene.

Total gas flow (NmL/min)	Type of graphene	%	I_D/I_G	I_{2D}/I_G	FWHM	G Raman shift (cm^{-1})	2D Raman shift (cm^{-1})	Thickness value
130	MONOLAYER	76.9	0.015	2.5	32	1580	2703	781
	BILAYER	11.4	0.016	1.4	47	1580	2699	
	FEW-LAYER	11.6	0.006	0.6	63	1580	2707	
	MULTILAYER	0.1	0.007	0.5	74	1581	2708	
100	MONOLAYER	78.5	0.032	1.5	56	1581	2699	798
	BILAYER	11.4	0.002	1.0	58	1580	2703	
	FEW-LAYER	9.9	0.002	0.5	69	1581	2711	
	MULTILAYER	0.2	0.006	0.5	79	1580	2708	
80	MONOLAYER	80.2	0.075	3.7	42	1580	2699	810
	BILAYER	8.4	0.019	2.1	47	1580	2714	
	FEW-LAYER	11.1	0.005	0.5	71	1580	2713	
	MULTILAYER	0.3	0.006	0.4	74	1580	2711	

(Synthesis conditions: 980°C, 1 min reaction time, CH_4/H_2 = 0.07 v/v, and 80–130 NmL (CH_4 + H_2)/min).

In general, I_D/I_G ratio values were very low for all of the samples synthesized with different total gas flows; this means that the synthesized samples had low amount of defects. As one would expect, I_{2D}/I_G ratios increased from the multilayer graphene to the monolayer graphene [33]. According to Havener et al. [34] the variation in I_{2D}/I_G values for the different types of graphene obtained for each total flow studied could be due to the coupling effect of the graphene layer. Smaller values of this relationship derivate in a stronger coupling of the graphene sheets. For the synthesized sample, the opposite effect that occurred for I_{2D}/I_G rate was observed for the FWHM parameter, which decreased from the multilayer graphene to the monolayer graphene [33]. All of these parameters are characteristic of the CVD-growth of graphene [35]. Furthermore, 2D and G position are located in the typical values of CVD-graphene [29].

A combination of Raman spectroscopy data and Excel-VBA results verified that the best results were obtained for the sample synthesized with a reaction time of 1 minute and a total flow of 80 NmL/min; this sample was considered the optimum material. Four characteristic Raman spectra of the optimum sample are shown in Figure 7 along with the corresponding 2D peak deconvolution for each type of graphene. The 2D peak deconvolutions of multilayer (a) and few-layer (b) graphene were fitted with two different peaks, which were similar to those corresponding to graphite. Bilayer graphene (c) was deconvoluted to four different contributions, whereas monolayer graphene (d) presented one single symmetrical peak [36].

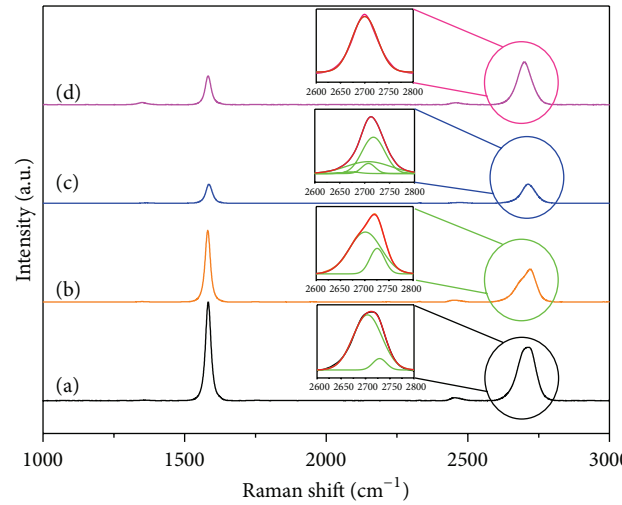

Figure 7: Raman spectra and 2D peak deconvolution corresponding to the optimized graphene sample (a) multilayer graphene, (b) few-layer graphene, (c) bilayer graphene, and (d) monolayer graphene (synthesis conditions: 980°C, 1 min reaction time, CH_4/H_2 = 0.07 v/v, 80 NmL (CH_4+H_2)/min).

4. Conclusions

The aim of the study reported here was to optimize the total gas flow applied during the reaction step for different reaction times using an atmospheric pressure Chemical Vapor Deposition set-up designed and fabricated at laboratory scale. Polycrystalline nickel was chosen as a cheap alternative to synthesize graphene rather than a single nickel crystal. H_2 and N_2 were used as carrier gases and CH_4 was used as the carbonaceous gas. Two synthesis parameters were studied in detail, namely, the total gas flow applied during the reaction step and the reaction time.

Four different colors, each of which is related to a particular type of graphene (monolayer, bilayer, few-layer, and multilayer), were observed. A maximum *thickness value* (810) was obtained with a temperature of 980°C, a CH_4/H_2 flow rate ratio of 0.07 v/v, a reaction time of 1 minute, and a total flow of 80 NmL/min. Under these conditions, about 80% of the polycrystalline nickel foil was covered with monolayer

graphene and the percentage of multilayer graphene over the sample was less than 1%.

Competing Interests

There are no competing interests related to this paper.

Acknowledgments

The authors gratefully acknowledge Spanish Ministry of Economy and Competiveness (Project CTQ2013-45030-R) for the financial support of this work.

References

[1] K. S. Novoselov, A. K. Geim, S. V. Morozov et al., "Electric field in atomically thin carbon films," *Science*, vol. 306, no. 5696, pp. 666–669, 2004.

[2] K. S. Novoselov, A. K. Geim, S. V. Morozov et al., "Two-dimensional gas of massless Dirac fermions in graphene," *Nature*, vol. 438, no. 7065, pp. 197–200, 2005.

[3] A. K. Geim and K. S. Novoselov, "The rise of graphene," *Nature Materials*, vol. 6, no. 3, pp. 183–191, 2007.

[4] A. K. Geim, "Graphene: status and prospects," *Science*, vol. 324, no. 5934, pp. 1530–1534, 2009.

[5] Y. Y. Wang, Z. H. Ni, T. Yu et al., "Raman studies of monolayer graphene: the substrate effect," *The Journal of Physical Chemistry C*, vol. 112, no. 29, pp. 10637–10640, 2008.

[6] Y. Zhu, S. Murali, W. Cai et al., "Graphene and graphene oxide: synthesis, properties, and applications," *Advanced Materials*, vol. 22, no. 35, pp. 3906–3924, 2010.

[7] K. E. Whitener Jr. and P. E. Sheehan, "Graphene synthesis," *Diamond and Related Materials*, vol. 46, pp. 25–34, 2014.

[8] M. I. Katsnelson, "Graphene: carbon in two dimensions," *Materials Today*, vol. 10, no. 1-2, pp. 20–27, 2007.

[9] C. Vallés, C. Drummond, H. Saadaoui et al., "Solutions of negatively charged graphene sheets and ribbons," *Journal of the American Chemical Society*, vol. 130, no. 47, pp. 15802–15804, 2008.

[10] K. S. Subrahmanyam, L. S. Panchakarla, A. Govindaraj, and C. N. R. Rao, "Simple method of preparing graphene flakes by an arc-discharge method," *Journal of Physical Chemistry C*, vol. 113, no. 11, pp. 4257–4259, 2009.

[11] Y. Chen, H. Zhao, L. Sheng et al., "Mass-production of highly-crystalline few-layer graphene sheets by arc discharge in various H_2-inert gas mixtures," *Chemical Physics Letters*, vol. 538, pp. 72–76, 2012.

[12] L. Jiao, L. Zhang, X. Wang, G. Diankov, and H. Dai, "Narrow graphene nanoribbons from carbon nanotubes," *Nature*, vol. 458, no. 7240, pp. 877–880, 2009.

[13] L. Valentini, "Formation of unzipped carbon nanotubes by CF4 plasma treatment," *Diamond and Related Materials*, vol. 20, no. 3, pp. 445–448, 2011.

[14] P. Blake, P. D. Brimicombe, R. R. Nair et al., "Graphene-based liquid crystal device," *Nano Letters*, vol. 8, no. 6, pp. 1704–1708, 2008.

[15] Y. Hernandez, V. Nicolosi, M. Lotya et al., "High-yield production of graphene by liquid-phase exfoliation of graphite," *Nature Nanotechnology*, vol. 3, no. 9, pp. 563–568, 2008.

[16] P. Sutter, "Epitaxial graphene: how silicon leaves the scene," *Nature Materials*, vol. 8, no. 3, pp. 171–172, 2009.

[17] M. P. Lavin-Lopez, J. L. Valverde, M. C. Cuevas et al., "Synthesis and characterization of graphene: influence of synthesis variables," *Physical Chemistry Chemical Physics*, vol. 16, no. 7, pp. 2962–2970, 2014.

[18] M. P. Lavin-Lopez, J. L. Valverde, A. Garrido, L. Sanchez-Silva, P. Martinez, and A. Romero-Izquierdo, "Novel etchings to transfer CVD-grown graphene from copper to arbitrary substrates," *Chemical Physics Letters*, vol. 614, pp. 89–94, 2014.

[19] G. A. López and E. J. Mittemeijer, "The solubility of C in solid Cu," *Scripta Materialia*, vol. 51, no. 1, pp. 1–5, 2004.

[20] G. Ruan, Z. Sun, Z. Peng, and J. M. Tour, "Growth of graphene from food, insects, and waste," *ACS Nano*, vol. 5, no. 9, pp. 7601–7607, 2011.

[21] Z. Sun, Z. Yan, J. Yao, E. Beitler, Y. Zhu, and J. M. Tour, "Growth of graphene from solid carbon sources," *Nature*, vol. 468, no. 7323, pp. 549–552, 2010.

[22] C. Mattevi, H. Kim, and M. Chhowalla, "A review of chemical vapour deposition of graphene on copper," *Journal of Materials Chemistry*, vol. 21, no. 10, pp. 3324–3334, 2011.

[23] M. P. Lavin-Lopez, J. L. Valverde, M. I. Ruiz-Enrique, L. Sanchez-Silva, and A. Romero, "Thickness control of graphene deposited over polycrystalline nickel," *New Journal of Chemistry*, vol. 39, no. 6, pp. 4414–4423, 2015.

[24] X. Li, W. Cai, J. An et al., "Large-area synthesis of high-quality and uniform graphene films on copper foils," *Science*, vol. 324, no. 5932, pp. 1312–1314, 2009.

[25] M. Wall, "Raman spectroscopy optimizes graphene characterization," *Advanced Materials and Processes*, vol. 170, no. 4, pp. 35–38, 2012.

[26] J. W. Suk, A. Kitt, C. W. Magnuson et al., "Transfer of CVD-grown monolayer graphene onto arbitrary substrates," *ACS Nano*, vol. 5, no. 9, pp. 6916–6924, 2011.

[27] A. Reina, X. Jia, J. Ho et al., "Large area, few-layer graphene films on arbitrary substrates by chemical vapor deposition," *Nano Letters*, vol. 9, no. 1, pp. 30–35, 2009.

[28] A. C. Ferrari, J. C. Meyer, V. Scardaci et al., "Raman spectrum of graphene and graphene layers," *Physical Review Letters*, vol. 97, no. 18, Article ID 187401, 2006.

[29] I. Calizo, D. Teweldebrhan, W. Bao, F. Miao, C. N. Lau, and A. A. Balandin, "Spectroscopic Raman nanometrology of graphene and graphene multilayers on arbitrary substrates," *Journal of Physics: Conference Series*, vol. 109, no. 1, Article ID 012008, p. 5, 2008.

[30] M. Losurdo, M. M. Giangregorio, P. Capezzuto, and G. Bruno, "Graphene CVD growth on copper and nickel: role of hydrogen in kinetics and structure," *Physical Chemistry Chemical Physics*, vol. 13, no. 46, pp. 20836–20843, 2011.

[31] A. Das, B. Chakraborty, and A. K. Sood, "Raman spectroscopy of graphene on different substrates and influence of defects," *Bulletin of Materials Science*, vol. 31, no. 3, pp. 579–584, 2008.

[32] C. N. R. Rao, U. Maitra, and H. S. S. R. Matte, *Synthesis, Characterization, and Selected Properties of Graphene*, Wiley-VCH, 2012.

[33] R. J. Nemanich and S. A. Solin, "First- and second-order Raman scattering from finite-size crystals of graphite," *Physical Review B*, vol. 20, no. 2, pp. 392–401, 1979.

[34] R. W. Havener, H. Zhuang, L. Brown, R. G. Hennig, and J. Park, "Angle-resolved raman imaging of interlayer rotations and interactions in twisted bilayer graphene," *Nano Letters*, vol. 12, no. 6, pp. 3162–3167, 2012.

[35] Y. Gong, X. Zhang, G. Liu et al., "Layer-controlled and wafer-scale synthesis of uniform and high-quality graphene films on a polycrystalline nickel catalyst," *Advanced Functional Materials*, vol. 22, no. 15, pp. 3153–3159, 2012.

[36] S. D. Costa, A. Righi, C. Fantini et al., "Resonant Raman spectroscopy of graphene grown on copper substrates," *Solid State Communications*, vol. 152, no. 15, pp. 1317–1320, 2012.